Numerical implementation of Einstein-Brillouin-Keller quantization for arbitrary potentials

Andrew J. Larkoski[a]
Department of Physics, University of Washington, Seattle, Washington 98105

David G. Ellis[b] and Lorenzo J. Curtis[c]
Department of Physics and Astronomy, University of Toledo, Toledo, Ohio 43606

The Einstein-Brillouin-Keller (EBK) quantization equation is used to determine the energy levels of a two-body system with an arbitrary central potential that allows for bound states. The treatment is based on the conservation laws and avoids both the Newtonian and Schrödinger differential equations. Because analytic solutions for the energy levels do not exist in general, the EBK condition is applied using the Newton-Raphson method and the radial probability density is computed. Potentials appropriate for a diatomic molecule are considered and the effect of the angular momentum on the radial distribution, the nature of the classical orbits, and the possibility of closed orbits is studied. © *2006 American Association of Physics Teachers.*
[DOI: 10.1119/1.2192788]

I. INTRODUCTION

The traditional approach to teaching undergraduate physics emphasizes problems that have relatively simple closed-form solutions. Even though the number of these exactly soluable problems is small, they allow an exposition of important mathematical methods. However, the application of these methods to more complex situations (such as perturbations or many-body interactions) is beyond the scope of an elementary course. Courses in introductory quantum mechanics also address problems with closed-form solutions. We shall show that the use of position probability densities allows classical and quantum mechanical approaches to be applied in a similar way to more complex situations by using numerical methods. Another advantage of placing more emphasis on numerical methods includes the fact that a wider class of problems can be treated.

In this paper we consider the two-body problem with an arbitrary central potential that allows for bound states. The treatment avoids both the Newtonian and Schrödinger formulations based on second-order differential equations and instead begins with conservation of energy and angular momentum. Given these quantities, the radial momentum, turning points, and position probability distribution are computed classically and quantization can be introduced using the Einstein–Brillouin–Keller (EBK) method.[1] As an example, potentials appropriate for a diatomic molecule are used.

II. CALCULATION

A. Two-body problem

We consider the classical two-body problem[2] with point masses m_1 and m_2 at positions r_1 and r_2 interacting through a central potential $U(r)$, where $r=r_1-r_2$ and $r=|r|$. When the center-of-mass motion is removed, the Lagrangian becomes

$$\mathcal{L} = \tfrac{1}{2}\mu\dot{r}^2 - U(r), \tag{1}$$

where the reduced mass is

$$\mu = \frac{m_1 m_2}{m_1 + m_2}. \tag{2}$$

The motion is confined to a plane, so we introduce polar coordinates r, ϕ, and write the angular momentum L as

$$L = \mu r^2 \dot{\phi} = \text{constant}. \tag{3}$$

The energy of the system is

$$E = \tfrac{1}{2}\mu\dot{r}^2 + \tfrac{1}{2}\mu r^2 \dot{\phi}^2 + U(r) = \tfrac{1}{2}\mu\dot{r}^2 + V_r, \tag{4}$$

where

$$V_r = \frac{1}{2}\frac{L^2}{\mu r^2} + U(r). \tag{5}$$

We can now consider the radial part of the two-body problem as equivalent to the problem of a particle of mass μ moving in one dimension with the effective potential V_r. It only remains to specify the central potential $U(r)$ to completely define the system.

The harmonic oscillator and Kepler-Coulomb potentials are well studied in both classical and quantum mechanics. To go beyond these exactly soluble cases, we consider the kind of radial potential used to model the motion of the nuclei in a diatomic molecule.

B. Model potentials

The Lennard-Jones (6-12) potential is a standard model potential for the interaction of two neutral atoms, including both bound[3] and scattering[4] states. It combines van der Waals attraction at large distances with a repulsive core. We take

$$U(r) = \frac{a}{r^{12}} - \frac{b}{r^6}, \tag{6}$$

where a and b are positive parameters. The value of the equilibrium separation r_0, which is the solution of $dU/dr=0$, is
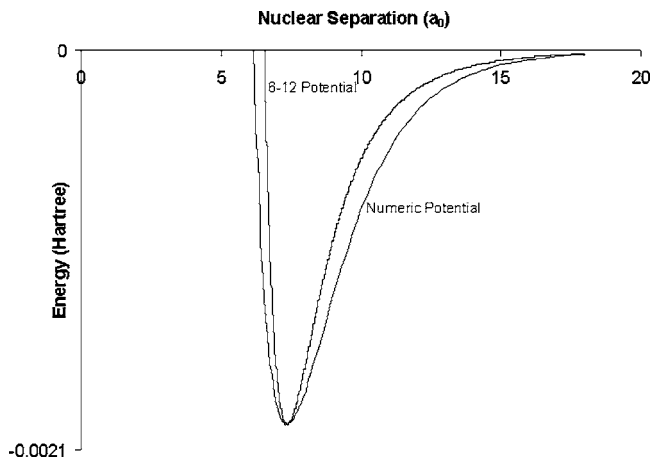
Fig. 1. Comparison of the potential (6-12) to the experimental tabulated potential.

$$r_0^6 = \frac{2a}{b}. \tag{7}$$

The value of the potential function at r_0 is

$$-\epsilon = \frac{b^2}{4a} - \frac{b^2}{2a} = -\frac{b^2}{4a}, \tag{8}$$

where ϵ is the magnitude of the depth of the potential evaluated at r_0. Thus, from Eqs. (7) and (8), the coefficients a and b are given by

$$a = \epsilon r_0^{12}, \quad b = 2\epsilon r_0^6. \tag{9}$$

The quantities ϵ and r_0 can be determined from experimentally measured values.

We use parameters[5] appropriate for the ground electronic state of the van der Waals molecule Mg_2: $\epsilon = 0.001\ 963\ 6$ hartree and $r_0 = 7.36$ bohr. In atomic units (hartree=bohr $= m_e = \hbar = 1$) $a = 4.96 \times 10^7$ and $b = 624$.

We also use a tabulated potential previously derived[6] for Mg_2, so that we will have comparable results and a programming check. Graphs comparing the analytic 6-12 potential to the tabulated potential are given in Fig. 1.

C. Energy eigenvalues

The energy eigenvalues of a quantum system can be determined using the EBK action quantization[7–9]

$$\frac{1}{2\pi} \oint p_i dq_i = \left(n_i + \frac{\mu_i}{4}\right)\hbar, \tag{10}$$

where the path integral is evaluated over the phase space of each coordinate q_i and its respective momentum p_i. In Eq. (10) n_i is a non-negative integer and μ_i is the Maslov index.[10] The latter represents the total phase loss during one period (in units of $\pi/2$). We refer to the discussions in Refs. 10 and 11 to justify the values of the Maslov index used in Eqs. (11) and (12), although we shall discuss the value for Eq. (11) in more detail.

The EBK quantization has been applied to several different systems, for example, the Kepler-Coulomb and isotropic oscillator potentials.[1] It yields accurate, sometimes exact, results for the energy levels and thus its use is often appropriate to avoid solving the Schrödinger equation.[11]

For a spherically symmetric potential, the quantization integrals for the zenith and azimuthal coordinates are[1]

$$\left(n_\vartheta + \frac{1}{2}\right)\hbar = \frac{1}{2\pi} \oint p_\vartheta d\vartheta = L - L_z, \tag{11}$$

$$n_\varphi \hbar = \frac{1}{2\pi} \oint p_\varphi d\varphi = L_z, \tag{12}$$

where ϑ and φ are the zenith and azimuthal angles, respectively, and L_z is the component of angular momentum along the z axis. If we combine Eqs. (11) and (12), we obtain

$$\left(n_\vartheta + n_\varphi + \tfrac{1}{2}\right)\hbar = L, \tag{13}$$

and thus

$$\left(\ell + \tfrac{1}{2}\right)\hbar = L, \tag{14}$$

with ℓ a non-negative integer. For large values of ℓ, we can see that

$$L^2 = \left(\ell^2 + \ell + \tfrac{1}{4}\right)\hbar^2 \cong \ell(\ell+1)\hbar^2. \tag{15}$$

The fact that the EBK quantization yields $L^2 = (\ell + 1/2)^2\hbar^2$ rather than the Schrödinger result $L^2 = \ell(\ell+1)\hbar^2$ is called the Langer modification and involves the automatic inclusion of a higher-order correction in the semiclassical formulation.[12] This modification has the effect of achieving the correct behavior for the uncorrected energies and wave functions near the singularity at $r=0$, although at the expense of the specification of the quantization of the angular momentum. As has been discussed by Watson,[13] the choice of whether or not to include the Langer modification is analogous to the choice of the zeroth-order solution in a perturbation calculation. For motions with a significant amplitude near $r=0$ (such as the Kepler-Coulomb or isotropic harmonic oscillator) the Langer form improves the zero-order energy (uncorrected near the $r=0$ singularity) and the EBK formulation gives a one-to-one correspondence between an eigenstate and the classical orbit. For the model potentials we are using, the amplitude near $r=0$ is small and there is no advantage to deviating from the traditional non-Langer form used in the analysis of vibrational-rotational spectra of diatomic molecules. Thus we shall use the familiar $\ell(\ell+1)$ form in Eq. (5) and its consequence in Eq. (17).

For a non-relativistic two-particle system in a potential, the radial momentum is given by

$$p_r = \sqrt{2\mu(E - V_r)}, \tag{16}$$

where E is the total energy, and V_r is the effective potential energy defined in Eq. (5). If we substitute Eq. (16) into Eq. (10), we can find the energy levels of the system. For the 6-12 potential, the momentum is

$$p_r = \sqrt{2\mu\left[E - \left(\frac{a}{r^{12}} - \frac{b}{r^6} + \frac{\ell(\ell+1)\hbar^2}{2\mu r^2}\right)\right]}. \tag{17}$$

The corresponding quantization is

$$\left(n_r + \frac{1}{2}\right)\hbar = \frac{1}{2\pi} \oint p_r dr = \frac{1}{\pi} \int_{r_1}^{r_2} p_r dr, \tag{18}$$

where p_r is defined in Eq. (16), n_r is the radial quantum number, and r_1 and r_2 are the radial periapsis and apoapsis, respectively.
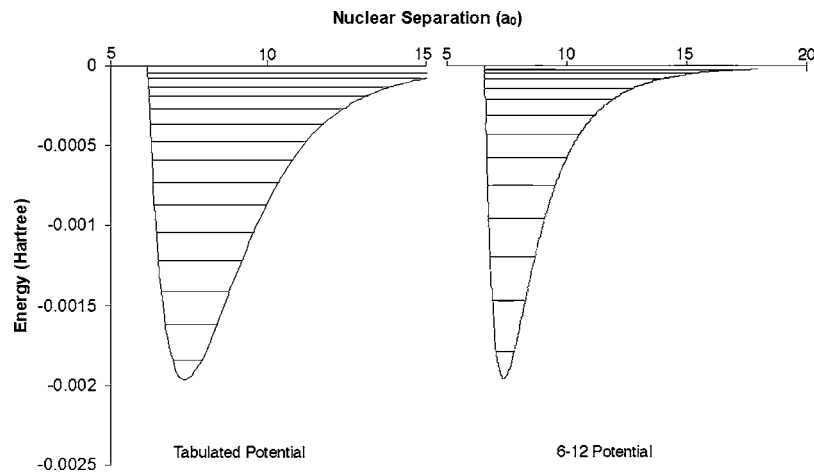
Fig. 2. The energy levels of the ground state of Mg_2 modeled by the 6-12 potential and the tabulated potential from Ref. 6.

Because no closed-form solution exists for the EBK quantization integral in Eq. (18) with p_r given by Eq. (17), we evaluated the integral numerically. For input values of n_r and ℓ, the program chooses an arbitrary initial value of E and uses Simpson's rule to calculate the integral. The program then iterates several times according to the Newton-Raphson method to find the energy that satisfies Eq. (18), adjusting both the total energy and the classical turning points corresponding to that energy. The calculated energy levels of the 6-12 potential that correspond to the ground electronic state of Mg_2 are illustrated in Fig. 2 and tabulated in Table I.

To calculate the energy levels of the ground electronic state of Mg_2 using the tabulated potential requires a few more steps. The program interpolates the potential for radial separations that are not in the table by a linear function joining two consecutive tabulated values. To evaluate Eq. (18) to find the energy eigenvalues (for given values of n_r and ℓ), the integral is numerically integrated, carefully taking into account the behavior at the end points. The results for the ground electronic state of Mg_2 are also illustrated in Fig. 2 and tabulated in Table I.

D. Probability distributions

The classical radial probability distributions associated with the calculated eigenvalues can be easily evaluated. The probability that the two atoms in the molecule are separated by a distance r is proportional to the inverse of the radial momentum. That is,

$$P(r)dr \propto \frac{dr}{p_r} = \frac{dr}{\sqrt{2\mu(E - V_r)}}.$$ (19)

The longer it takes the atoms to go from r to $r+dr$, the smaller the velocity and hence the higher the probability of finding the system in this configuration. As in quantum mechanics, the total probability of finding the system with any nuclear separation must be unity.

Classical probabilities have been evaluated for both the 6-12 (Fig. 3) and numerical (Figs. 3 and 4) potentials. For small values of n_r, the curve is similar to a harmonic potential probability distribution (all potential wells can be represented by a harmonic potential near the potential minimum). For larger values of n_r (Fig. 4), the distribution is no longer like the harmonic oscillator, and is asymmetric. Notice that at the close-separation turning point, where the slope of the

Table I. Energy levels of the ground electronic state of Mg_2 modeled by a 6-12 and tabulated potentials; 1 hartree = 27.212 eV = 219 474.6 cm^{-1}.

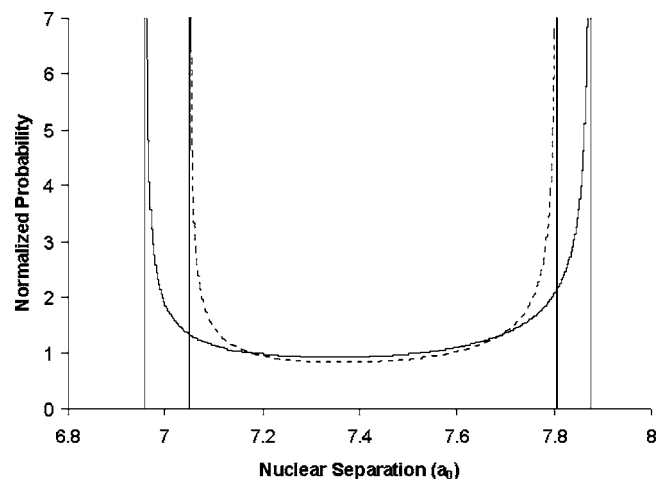|	6-12		Tabulated	
n_r	Energy (Hartree)	Energy (cm^{-1})	Energy (Hartree)	Energy (cm^{-1})
0	−0.001 792	−393.334 70	−0.001 844	−404.809 93
1	−0.001 479	−324.526 78	−0.001 621	−355.698 09
2	−0.001 202	−263.896 04	−0.001 411	−309.753 28
3	−0.000 961	−211.021 16	−0.001 219	−267.442 97
4	−0.000 754	−165.462 87	−0.001 041	−228.407 22
5	−0.000 578	−126.762 71	−0.000 877	−192.419 09
6	−0.000 430	−94.441 50	−0.000 727	−159.448 74
7	−0.000 310	−67.998 21	−0.000 591	−129.738 24
8	−0.000 214	−46.908 66	−0.000 470	−103.252 70
9	−0.000 140	−30.624 50	−0.000 363	−79.759 48
10	−0.000 085	−18.572 47	−0.000 271	−59.396 85
11	−0.000 046	−10.154 04	−0.000 192	−42.219 23
12	−0.000 022	−4.745 78	−0.000 130	−28.499 65
13			−0.000 080	−17.465 70
14			−0.000 043	−9.521 47

Fig. 3. Classical probability distribution for a low quantum state using the 6-12 potential (dotted curve) and the tabulated potential (solid curve).
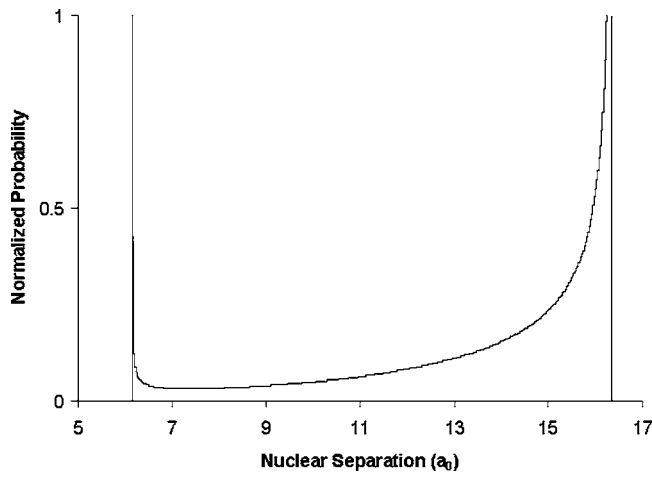
Fig. 4. Classical probability distribution for a high quantum state evaluated from the numerical potential.

Fig. 5. Comparison of the effective potentials of different angular momenta for the 6-12 model.

potential is very large, the probability density rapidly increases, while at the far-separation turning point, where the slope of the potential is very small, the probability density increases more slowly. This behavior is reasonable because the radial momentum is changing very quickly where the potential is changing quickly and slowly where the potential is less steep.

The calculated probability distributions for the 6-12 and the tabulated potentials allow us to calculate expectation values for various radial quantum numbers. The classical expectation value $\langle r^n \rangle$ for an integer n is given by

$$\langle r^n \rangle = \int_{-\infty}^{\infty} r^n P(r) dr, \qquad (20)$$

where $P(r)$ is the normalized probability. For a semiclassical diatomic molecule, the bounds of integration extend from one turning point to the other because the probability of tunneling outside the potential is zero (a quantum mechanical treatment requires infinite bounds). Table II lists several expectation values for both potentials for various quantum numbers.

E. Effect of angular momentum

The effective potential V_r depends on the angular momentum [see Eq. (5)]. For small values of ℓ the potential is affected only slightly because the centrifugal term is much

less than $U(r)$ (the reduced mass in the denominator for Mg_2 is about $21\,000\ m_e$). For higher values of ℓ, there is an appreciable change as illustrated in Fig. 5 for $\ell=0$ and $\ell=26$, using the 6-12 potential. As a result of the change in the effective potential, the energy levels are affected as is evident in Table III. The effect of the angular momentum on the energy levels of the numerical potential is illustrated in Fig. 6. As ℓ increases for the same value of n_r, the energy level separation increases as ℓ^2, exhibiting that rotational effects are not negligible even at room temperature energies ($\approx 1/40$ eV) or an angular momentum of only $10\hbar$ for $n_r =4$ for the case of Mg_2.

III. CLASSICAL ATOMIC ORBITS

The classical orbit of the two atoms in a diatomic molecule can be found using the same methods as were used to solve the two-body problem. From Eq. (3) the angular velocity $\dot{\phi}$ is then

$$\dot{\phi} = \frac{L}{\mu r^2}. \qquad (21)$$

A differential equation for $d\phi/dr$ can be written as[2]

Table II. Expectation values for different energy levels for the 6-12 potential and the tabulated potential. Measured in units of Bohr radii[n].

n_r	$\langle r^n \rangle$	6-12	Tabulated
10	r^{-1}	0.085 716 6	0.098 163 9
10	r^1	12.082	10.666 6
10	r^2	149.861	117.755
11	r^{-1}	0.077 873 4	0.093 237 3
11	r^1	13.350 4	11.270 6
11	r^2	183.286	131.637
12	r^{-1}	0.068 881 8	0.088 746 6
12	r^1	15.148 7	11.939 4
12	r^2	236.293	148.301

Table III. Comparison of energy levels in the 6-12 and tabulated potentials. Energy in hartrees.

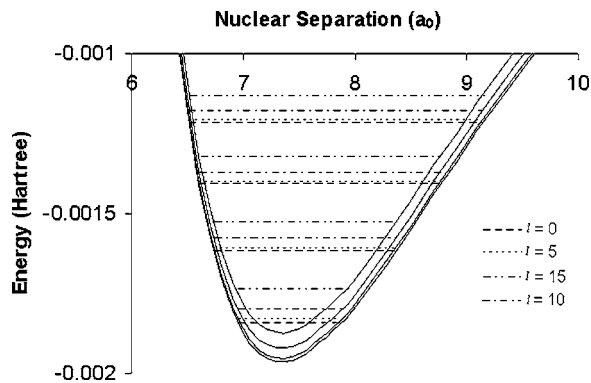| n_r | 6-12 | | Tabulated | |
	Energy ($\ell=0$)	Energy ($\ell=26$)	Energy ($\ell=0$)	Energy ($\ell=19$)
0	−0.001 792	−0.001 492	−0.001 844	−0.001 77
1	−0.001 479	−0.001 193	−0.001 621	−0.001 51
2	−0.001 202	−0.000 932	−0.001 411	−0.001 3
3	−0.000 961	−0.000 707	−0.001 219	−0.001 11
4	−0.000 754	−0.000 516	−0.001 041	−0.000 93
5	−0.000 578	−0.000 357	−0.000 877	−0.000 77
6	−0.000 43	−0.000 229	−0.000 727	−0.000 63
7	−0.000 31	−0.000 128	−0.000 591	−0.000 5
8	−0.000 214	−0.000 052	−0.000 47	−0.000 38

Fig. 6. Comparison of the effective potentials and energy levels of the tabulated potential with varying angular momenta. The lowest potential curve corresponds to $\ell=0$, the next, the $\ell=5$ state and so on.

Table IV. The fraction of one complete revolution traversed between two successive transits through a given turning point for the two potentials discussed in the text. These fractions indicate degree of precession of the non-closed orbit.

n_r	ℓ	6-12	Tabulated
0	1	0.002 572	0.003 801
0	25	0.066 345	0.113 63
8	8	0.046 039	0.040 746
12	15	0.294 944	0.121 137
14	1	0.031 534	0.009 785

$$\frac{d\phi}{dr} = \frac{d\phi}{dt}\frac{dt}{dr} = \frac{\dot{\phi}}{\dot{r}},\tag{22}$$

and thus we can solve for ϕ as a function of r as

$$\phi(r) = \int \frac{\dot{\phi}}{\dot{r}}dr = \int \frac{L}{r^2}\frac{dr}{\sqrt{2\mu(E-V_r)}}.\tag{23}$$

For a closed orbit to exist, the angular difference between two successive transits through a given turning point must be a rational fraction times 2π (that is, after a finite number of oscillations between the turning points, the orbit will exactly repeat itself). This condition can be expressed as[2]

$$\frac{a}{b}2\pi = \oint \frac{L}{r^2}\frac{dr}{\sqrt{2\mu(E-V_r)}},\tag{24}$$

where a and b are nonzero integers (a is allowed to be zero, but this value corresponds to zero angular momentum, which is not interesting). The ratio a/b is the fraction of a full revolution (2π rad) that the orbit completes between two successive transits through a given turning point. After b such oscillations, the orbit closes on itself. The integral is readily evaluated for an arbitrary central potential using the numerical methods described in Sec. II.

For a central potential $U(r) \propto r^n$, with n an integer, a non-circular, closed orbit exists only for $n=-1$ and 2, corresponding to a Kepler-Coulomb potential and the harmonic potential, respectively.[2] For a diatomic molecule, it is not appropriate to estimate the orbits using these potentials (especially the harmonic oscillator for low quantum numbers). However, the potential in a diatomic molecule is not proportional to an integer power of the internuclear separation, so closed orbits are not guaranteed.

The closed orbit integral in Eq. (24) was evaluated for many interesting cases, which are listed in Table IV; one case is plotted in Fig. 7. Note that these orbits are not closed, because in general the radial and angular periods are not commensurate. As illustrated in a recent review of Einstein's early work,[14] the orbits do not satisfy the ergodic hypothesis, that is, the trajectory does not uniformly cover all available phase space. Although every allowed spatial point is reached, at each point the radial momentum has only one of two possible values. The system point in phase space moves on the surface of an invariant torus,[15] with the outward motion in Fig. 7 corresponding to the upper surface and the inward motion to the lower.

IV. CONCLUSION

The bound-state two-body problem was solved numerically using two central potentials, one analytic and one numerical. No approximations were used, except for the numerical evaluation of various integrals.

The energy levels and average powers of r tabulated here provide the basis for a realistic conceptual model of a molecular potential. Moreover, the position probability densities from which they were computed can be used to extend the model through energy perturbation or level overlap calculations. This approach has advantages over the common formulation in which a molecular potential is modeled as a one-dimensional simple harmonic oscillator perturbed by a Morse potential, which is expanded as a power series in the displacement from equilibrium $x=r-r_0$. In the one-dimensional simple harmonic oscillator formulation the unperturbed model has equally spaced energy levels and is symmetric about the equilibrium. The perturbation alters the equal spacing, but does not remove the symmetry about the equilibrium point because only even powers of x are nonvanishing in this basis. In the numerical formulation we have applied these features are already present in the unperturbed system.
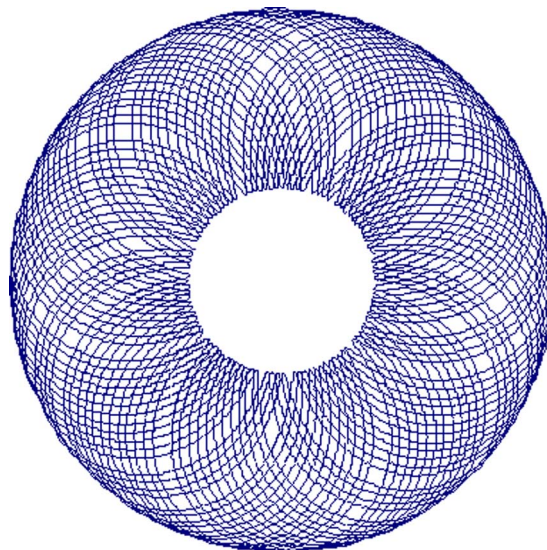

Fig. 7. Orbit in a 6-12 potential with $n_r=12$ and $\ell=15$.

The methods can be used in an undergraduate course and provide insights into the types of approximation strategies used in current research. It is simple to extend the non-relativistic analysis to the relativistic realm. As is outlined in Ref. 1, the radial momentum can be solved for from the relativistic expression

$$E + mc^2 = \sqrt{p^2c^2 + m^2c^4} + U(r), \qquad (25)$$

and

$$p^2c^2 = \left(p_r^2 + \frac{L^2}{r^2}\right)c^2, \qquad (26)$$

where L is a discrete multiple of $\hbar$. We need only to solve for p_r and substitute the result into Eq. (10) to determine the allowed energy levels for an arbitrary $U(r)$.

ACKNOWLEDGMENT

[a] Electronic mail: larkoa@u.washington.edu
[b] Electronic mail: dge@physics.utoledo.edu
[c] Electronic mail: ljc@physics.utoledo.edu

[1] Lorenzo J. Curtis and David G. Ellis, "Use of the Einstein-Brillouin-Keller action quantization," Am. J. Phys. **72**, 1521–1523 (2004).
[2] Jerry B. Marion and Stephen T. Thornton, *Classical Dynamics of Particles and Systems* (Saunders C.P., New York, 1995), 4th ed., pp. 291–301.
[3] J. E. Kilpatrick and M. F. Kilpatrick, "Discrete energy levels associated with the Lennard-Jones potential," J. Chem. Phys. **19**, 930–933 (1951).
[4] M. R. Flannery, "Elastic scattering," in *Atomic, Molecular, and Optical Physics Handbook*, edited by G. W. F. Drake (AIP, New York, 1996), p. 520.
[5] W. J. Balfour and A. E. Douglas, "Absorption spectrum of the Mg_2 molecule," Can. J. Phys. **48**, 901–914 (1970).
[6] "Potential energy surface database of group II dimer molecules," ⟨physics.nist.gov/PhysRefData/PES/RefData/Mg.html⟩.
[7] A. Einstein, "Zum Quantensatz von Sommerfeld und Epstein," Verh. Dtsch. Phys. Ges. **19**, 82–92 (1917).
[8] L. Brillouin, "Remarques sur la mécanique ondulatoire," J. Phys. Radium **7**, 353–368 (1926).
[9] J. B. Keller, "Corrected Bohr-Sommerfeld quantum conditions for non-separable systems," Ann. Phys. (N.Y.) **4**, 180–188 (1958).
[10] V. P. Maslov, *Théorie des Perturbations et Methods Asymptotiques* (Denod Gauthier-Villars, Paris, 1972).
[11] Lorenzo J. Curtis, *Atomic Structure and Lifetimes: A Conceptual Approach* (Cambridge U. P., Cambridge, 2003).
[12] R. E. Langer, "On the connection formulas and the solutions of the wave equations," Phys. Rev. **51**, 669–676 (1937).
[13] J. K. G. Watson, "Semiclassical quantization and the Langer modification," J. Chem. Phys. **90**, 6443–6448 (1989).
[14] A. Douglas Stone, "Einstein's unknown insight and the problem of quantizing chaos," Phys. Today **58**(8), 37–43 (2005).
[15] E. Tannenbaum and E. J. Heller, "Semiclassical quantization using invariant tori: A gradient descent approach," J. Phys. Chem. A **105**, 2803–2813 (2001).

RELATIVITY: A THEORY OF DESCRIPTIONS

Einstein's great contribution was to show that there are certain features of their own states of motion that observers would never be able to measure (which is just what we mean by symmetry), and therefore these features could not and should not play a role in the observers' description of reality. The features do not destroy the equivalence of the observers. If you can't measure it, it mustn't enter into the story you are telling (at least in physics; literature is another matter entirely), and if it is not in your story, it can't be used to distinguish you from any other observer. In short, relativity is a theory of descriptions. More correctly, it is a theory of the relationships between descriptions and the equivalence of descriptions.

Morton Tavel, *Contemporary Physics and the Limits of Knowledge* (Rutgers, 2002), p. 7.